Effect of tethered chains on adhesion

Scott W. Sides, Gary S. Grest, and Mark J. Stevens
Sandia National Laboratories, Albuquerque, New Mexico 87185-1411
(October 27, 2000)

We study adhesion enhancement between a polymer melt and substrate due to chemically attached chains on the substrate surface. We have performed extensive molecular dynamics simulations to study the effect of temperature, crosslink density, tethered chain density (Σ), tethered chain length (N_g) and tensile pull-velocity (v) on the adhesion failure mechanisms of pull-out and/or scission of the tethered chains. We observe a crossover from pure chain pull-out at short N_g and small v, to chain scission as N_g and v are increased. The value of N_g for which this crossover occurs is comparable to the entanglement length.

Adhesion at polymer interfaces is relevant in either the mixing of two immiscible homopolymers (A+B) or attaching a homopolymer melt to a hard surface (A+substrate). In both cases, the addition of a third component can increase the entanglements at a polymer interface. For the first case, the extra component is a block copolymer made of the A and B species. For the latter case, the extra component is a layer of the A species which is chemically end-graphed onto the substrate. These tethered polymer layers, or brushes are relevant in such applications as colloidal stabilization [1,2], filler modification of polymeric materials and lubrication [3]. Substrate-tethered polymers can also increase adhesion enhancement, i. e. the mechanical work needed to break an adhesive bond.

Two key parameters characterizing this system are the length (N_g) and the areal density (Σ) of the tethered chains. Adhesion enhancement due to a tethered polymer layer shows a surprising non-monotonic behavior as a function of N_g and Σ. The work of adhesion first increases for small values of N_g and Σ, then decreases once either of these parameters is increased beyond a critical value due to the phase behavior of the end-tethered chains in contact with a long polymer melt [4–7]. This non-monotonic behavior has been observed by Kramer and co-workers in glassy polymers [8–12] and Léger and co-workers in elastomeric materials [7,13]. However, the interplay between the microscopic failure mechanisms of tethered chain pull-out, scission and crazing are not fully understood, partly due to the difficulty of direct experimental observation of these phenomena. Molecular dynamics (MD) simulations of fracture in highly crosslinked systems [14] and crazing [15,16] have helped to elucidate the crossover from adhesion to cohesive failure of polymer adhesives near walls *without* end-tethered chains. Simulations of tethered chains on small, highly simplified models in 2D have been performed [17,18], but were unable to study the effects of chain scission in particular. In this letter we present the first, large-scale simulations to study the adhesion failure mechanisms of end-tethered chains in contact with an entangled polymer melt.

We perform continuous-space, molecular dynamics (MD) simulations on a coarse-grained model of polymer chains. The polymers are represented by attaching N spherical beads of mass m with a finitely extensible spring. Bead trajectories are obtained by stepwise integration of Newton's equations of motion (EOM) which include terms for a weak stochastic force and a viscous drag force with a coefficient on the viscous force term of $0.5\tau^{-1}$ [19]. The addition of these two forces to the EOM effectively couples the system to a heat bath. The EOM for each particle is integrated with a velocity-Verlet [20] algorithm with a time step Δt=0.006τ, where $\tau=\sigma(m/\epsilon)^{1/2}$, with σ and ϵ setting the length and energy scales respectively. Each nonbonded pair of monomers interacts through a standard (12-6) Lennard-Jones interaction $U_{\rm LJ}(r)$, truncated at r_c=2.2σ.

To study the effect of chain scission on adhesion, the standard finite extensible non-linear elastic (FENE) potential [19] is altered to allow for broken bonds along a polymer chain. The bonding potential, $U_{\rm b}(r)$, between two adjacent beads a distance r apart on the same chain takes the form

$$U_{\rm b}(r) = \begin{cases} U_{\rm LJ}(r) + kr^4\left[(r-r_1)(r-r_2)\right] + U_c & r < r_{\rm br} \\ 0 & r > r_{\rm br} \end{cases}$$

with $r_{\rm br}$ the length at which a bond along the chain is considered broken. This form allows for two extrema in the bond potential; one stable, global minimum near the LJ potential energy minimum, and one local maximum near $r_{\rm br}$ where the bond force becomes zero. This allows bonds to be removed safely from the force calculation without causing large recoil velocities on the resulting chain ends. The remaining parameters in $U_{\rm b}(r)$ are k=$-409.12\epsilon/\sigma^6$, r_1=1.2σ, r_2=1.219σ and U_c=42.059ϵ which result from fitting $U_{\rm b}(r)$ to a standard FENE potential such that $r_{\rm br}$=1.21σ and the barrier to bond breaking is $\Delta U_{\rm b} \approx 20 k_{\rm B}T$.

Several factors need to be considered to construct and equilibrate appropriate starting states. To avoid the difficulties in constructing the correct chain configurations

for the various wet brush regimes we restrict the present study to areal densities Σ in the so-called "mushroom regime" [4,5]. In this regime each tethered chain does not interact directly with other tethered chains and may be constructed as a Gaussian chain. So, for each system of a given N_g and Σ, all chains are constructed as random walks with the correct radius of gyration and the tethered chains are attached to the substrate wall in random locations. A soft potential is used to remove overlaps and the size of the simulation cell is adjusted until the pressure $P \approx 0$ resulting in an overall monomer density of $\rho \approx 0.85\sigma^{-3}$. For all simulations, the length of the melt chains is N_m=2500 and the number of tethered chains is n_g=30. Most of the simulations are performed with T=1.0ϵ/k_B, which is well above the glass transition temperature T_g=0.5 − 0.6ϵ/k_B [15]. Simulations are performed using the massively parallel MD code LAMMPS [21], developed at Sandia and run on the ASCI Red Teraflop machine and Computational Plant (Cplant) clusters.

Figure 1 shows chain configurations at different times from a tensile pull simulation consisting of approximately 2×10^5 particles with N_g=250. Our largest systems contain $\approx 10^6$ particles. The Raster3D [22] software package is used to render the chain configurations shown in Fig. 1. The tensile pull is achieved by moving only the bottom wall every ten timesteps, as shown in Fig. 1. The tethered chains are attached to the bottom wall of the simulation cell and the top wall has no chains attached. For speed and simplicity, the wall interaction with the chains is modeled as an integrated LJ potential. The interaction strength of the top wall is set to be sufficiently strong so that no adhesive failure occurs on the top wall during pulling. The interaction of the bottom wall with the melt has a very weak attractive component, so that the adhesion enhancement due to the tethered chains may be studied independently of the adhesion to the bare wall. The z axis is normal to both walls and periodic boundary conditions are used in the x and y directions. The size of the simulation cell in the z direction is set to be approximately three times the radius of gyration of the tethered chains prior to pulling. The red chains are tethered, blue chains represent the entangled melt and green chains were initially tethered and have since broken. The three snapshots illustrate a failure mechanism for a system near the crossover between pure chain pull-out and chain scission. The tethered chains in Fig. 1 are sufficiently long to be entangled with the polymer melt such that the relaxation time for the tethered chains is longer than the time scale imposed by the velocity of the moving wall. For a given v and T, longer tethered chains pull-out a comparable amount before breaking. More quantitative measures of chain scission and its dependence on N_g and v are given in Fig. 4.

During a pull simulation we measure the remaining length of the tethered chains and the work done by the

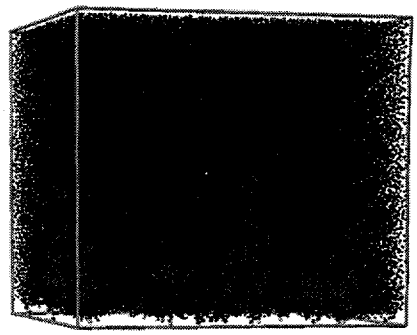

FIG. 1. Chain configurations at three times during a tensile pull simulation with T=1.0ϵ/k_B and pull velocity v=0.167 $\sigma\tau^{-1}$. The elapsed times shown are 60τ, 720τ and 960τ respectively. The red monomers belong to tethered chains and blue monomers belong to melt chains. Green monomers belong to sections of tethered chains which are no longer attached to the bottom substrate. The tethered chains shown here are N_g=250 and Σ=0.008σ^{-2}.

bottom wall. Figure 2 shows the integrated work over time W_t, as a function of time for different values of N_g. The data shown in Fig. 2 are for v=0.0167σ τ^{-1}, T=1.0ϵ/k_B and Σ=0.008σ^{-2}. For each tethered chain length, W_t is plotted for a sufficiently long time such that the tethered chains have either completely pulled out or each of the attached chains has broken. The turnover in the work for each N_g signifies the complete de-bonding of the pulling surface from the entangled melt. For the larger N_g the slope in W_t does not vanish because finite work is done pulling the remaining parts of the tethered chains due to the presence of an effective solvent as a result of the heat bath algorithm in the EOM. Clearly, surfaces with longer tethered chains require more work to completely pull away from the adjacent polymer melt than do short chains. However, for the same values of T and v the amount of work done in pulling chains out of the melt is nearly identical at short times. This suggests a chain-independent friction coefficient. Various theories [18,23] have suggested a power-law dependence for the work of adhesion of the form, N_g^α, where $1 \geq \alpha \geq 2$. Simulations on simplified models of pull-out have suggested that α=1 for small N_g and crosses over to α=3/2 for longer chains. The data in Fig. 2 shows a linear dependence in W_t for short chains and a greater than linear dependence for longer chains. However, the longest tethered chain lengths N_g=350 and 500 suggest that the amount of work begins to saturate for very long chains. This observation is consistent with the conclusions on the chain breaking data presented in Fig. 4.

Figure 3 shows the effect of varying temperature on W_t. The data shown in Fig. 3 are for v=0.0167σ τ^{-1}, Σ=0.008σ^{-2} and N_g=250. Figure 3 compares data for temperatures below, near and above T_g. The slope of W_t for T=0.3ϵ/k_B is significantly larger than the rest of

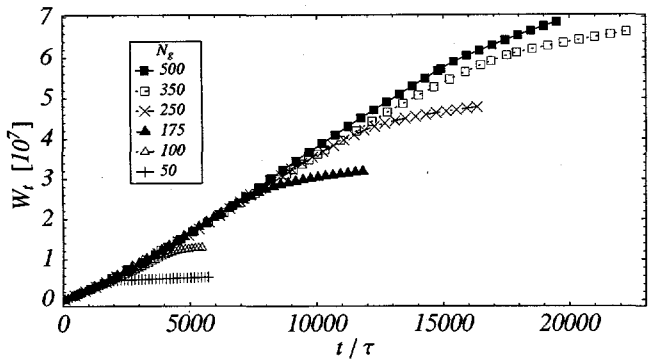

FIG. 2. Total integrated work vs. time for different tethered chain lengths. All data shown are for v=0.0167σ τ^{-1}, T=1.0ϵ/k_B and Σ=0.008σ^{-2}.

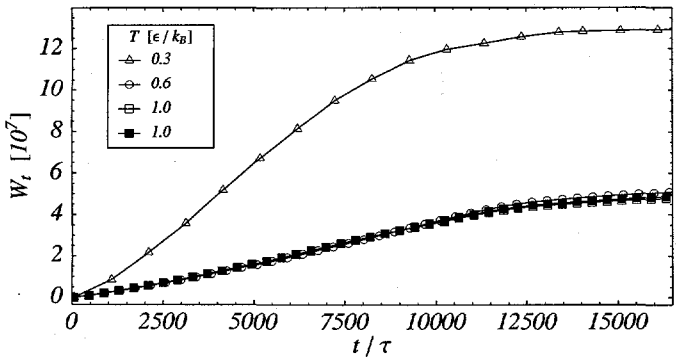

FIG. 3. Total integrated work vs. time for for three different temperatures. All open/filled symbol(s) denote uncrosslinked/crosslinked system(s). The data shown are all for v=0.0167σ τ^{-1}, Σ=0.008σ^{-2} and N_g=250.

the data for $T \geq 0.6\epsilon/k_B$. This suggests a friction coefficient that dramatically increases as the temperature is reduced below T_g. Also, the average length of the broken tethered chains still attached to the wall is significantly reduced as T is reduced. The open symbols in Fig. 3 denote uncrosslinked systems while the filled symbol denotes a system crosslinked at an average distance between crosslinks of 70 monomers. For the data in this letter, as well as the data to be presented in a more detailed paper, crosslinking appears to have little effect on W_t. This is likely due to the fact that the pulling wall is strongly repulsive and unable to initiate any crazing in the polymer melt.

The main result of this letter is illustrated in Fig. 4, which shows the fractional average length of remaining tethered chains $\langle F_g \rangle$ versus tethered chain length N_g. If

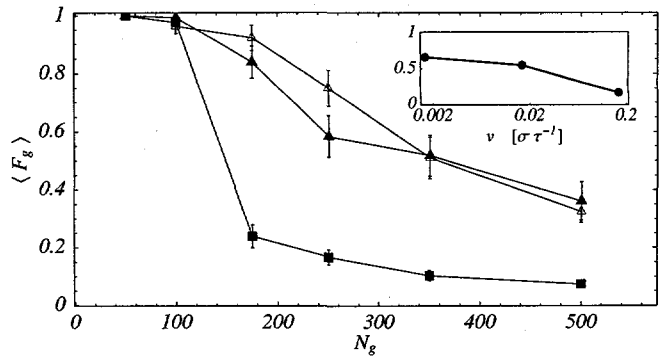

FIG. 4. Fractional average length of remaining tethered chains $\langle F_g \rangle$ vs. initial tethered chain length N_g. The data shown are all for uncrosslinked systems at T=1.0ϵ/k_B. The plotting symbols denote v=0.167$\sigma\tau^{-1}$, Σ=0.008σ^{-2} (filled square), v=0.0167$\sigma\tau^{-1}$, Σ=0.008σ^{-2} (filled triangle), and v=0.0167$\sigma\tau^{-1}$, Σ=0.002σ^{-2} (open triangle). Inset: $\langle F_g \rangle$ vs. tensile pull velocity v for T=1.0ϵ/k_B, N_g=250 and Σ=0.008σ^{-2}.

$N_g^i(t_f)$ is defined to be length of the ith tethered chain at the end of a pull simulation then

$$\langle F_g \rangle = \frac{\Sigma_i^{n_g} N_g^i(t_f)/n_g}{N_g} .$$

The value of $\langle F_g \rangle$ quantifies the length of the tethered chains still attached to the surface at the end of a pull. F=1 corresponds to pure chain pull-out and F=0 to pure chain scission. The filled symbols in Fig. 4 represent data for two velocities at Σ=0.008σ^{-2} and show an adhesion failure mechanism of almost pure chain pull-out for $N_g \leq 100$. For $N_g \sim 100$ there is a crossover to a failure mechanism with greater amounts of chain scission as N_g increases. The entanglement length calculated from the plateau modulus for this model has been estimated by Pütz et al. [24] to be $N_e \approx 74$. Thus, the crossover value corresponds to approximately $1.5N_e$. However other calculations [25] suggest that N_e may increase in the vicinity of a hard wall. In addition, the crossover occurs more rapidly at the faster pulling rate. The rate dependence of chain scission is further illustrated by the inset in Fig. 4 which shows $\langle F_g \rangle$ over three decades in pulling velocity. The amount of chain scission clearly decreases with decreasing pull velocity. The open triangles in Fig. 4 represent data for v=0.0167$\sigma\tau^{-1}$ at a smaller areal density Σ=0.002σ^{-2}. This data confirms our estimates for values of Σ which place the system in the "mushroom regime". Once the areal density of tethered chains is sufficiently low so that none of the chains can interact, the amount of chain scission is the same for all Σ.

In conclusion, we performed the first large-scale MD simulations to study the effects of end-tethered chains on adhesion in a 3D, realistic polymer model. Data is

presented which illustrates a crossover from pure chain pull-out to increasing chain scission which depends on N_g and v. The value of N_g for which this crossover occurs is near the chain entanglement length for this model. Experiments on the fracture properties of glassy polymers reinforced by block copolymer additives report a large increase in the work of adhesion when the molecular weight of the copolymer increases beyond the entanglement length. However, the data suggest this increase is due to crazing which is not seen in our simulations because the wall interaction is relatively weak. Further work is needed to investigate the effect of tethered chains specifically on crazing mechanisms and the possible roles of chain pull-out and scission on craze failure. Work is proceeding to extend simulations to include non-zero bond bending and torsional interactions as well as realistic potentials for adhesives like PDMS.

Sandia is a multiprogram laboratory operated by Sandia Corporation, a Lockheed Martin Company, for the United States Department of Energy under Contract DE-AC04-94AL85000.

[1] D. H. Napper, *Polymeric Stabilization of Colloidal Dispersions* (Academic, London, 1983).
[2] W. B. Russell, D. A. Saville, and W. R. Schowalter, *Colloidal Dispersions* (Cambridge University Press, Cambridge, 1989).
[3] J. Klein, Ann. Rev. Mat. Sci. **26**, 581 (1996).
[4] P. G. deGennes, Macromolcules **13**, 1069 (1980).
[5] M. Aubouy, G. H. Fredrickson, P. Pincus, and E. Raphaël, Macromolecules **28**, 2979 (1995).
[6] G. S. Grest, J. Chem. Phys. **105**, 5532 (1996).
[7] L. Léger, E. Raphaël, and H. Hervet, in *Advances In Polymer Science*, edited by S. Granick (Springer, Berlin, 1999), Vol. 138, p. 185.
[8] C. Creton, E. J. Kramer, and G. Hadziioannou, Macromolecules **24**, 1846 (1991).
[9] J. Washiyama, E. J. Kramer, C. F. Creton, and C.-Y. Hui, Macromolecules **27**, 2019 (1994).
[10] E. J. Kramer *et al.*, Faraday Discuss. **98**, 31 (1994).
[11] L. Norton *et al.*, Macromolecules **28**, 1999 (1995).
[12] C.-A. Dai, E. J. Kramer, J. Washiyama??, and C.-Y. Hui, Macromolecules **29**, 7536 (1996).
[13] M. Deruelle, L. Léger, and M. Tirrell, Macromolecules **28**, 7419 (1995).
[14] M. J. Stevens, Macromolecules, in press .
[15] A. R. C. Baljon and M. O. Robbins, Science **271**, 482 (1996).
[16] D. Gersappe and M. O. Robbins, Euro. Phys. Lett. **48**, 150 (1999).
[17] G. T. Pickett, D. Jasnow, and A. C. Balazs, Phys. Rev. Lett. **77**, 671 (1996).
[18] M. Sabouri-Ghomi, S. Ispolatov, and M. Grant, Phys. Rev. E **60**, 4460 (1999).
[19] K. Kremer and G. S. Grest, J. Chem. Phys. **92**, 5057 (1990).
[20] M. Allen and D. Tildesley, *Computer Simulation of Liquids* (Clarendon, Oxford, 1987).
[21] S. Plimpton, J. Comp. Phys. **117**, 1 (1995).
[22] E. A. Merritt and D. J. Bacon, Meth. Enzymol. **277**, 505 (1997).
[23] E. Raphaël and P. G. deGennes, J. Phys. Chem. **96**, 4002 (1992).
[24] M. Pütz, K. Kremer, and G. S. Grest, Euro. Phys. Lett. **49**, 735 (2000), The simulations in this paper used a purely repulsive interaction between non-bonded monomers and a FENE interaction between bonded monomers. The N_e for this model is expected to be very similiar to that of the model used in the present study.
[25] H. R. Brown and T. P. Russell, Macromolecules **29**, 798 (1996).

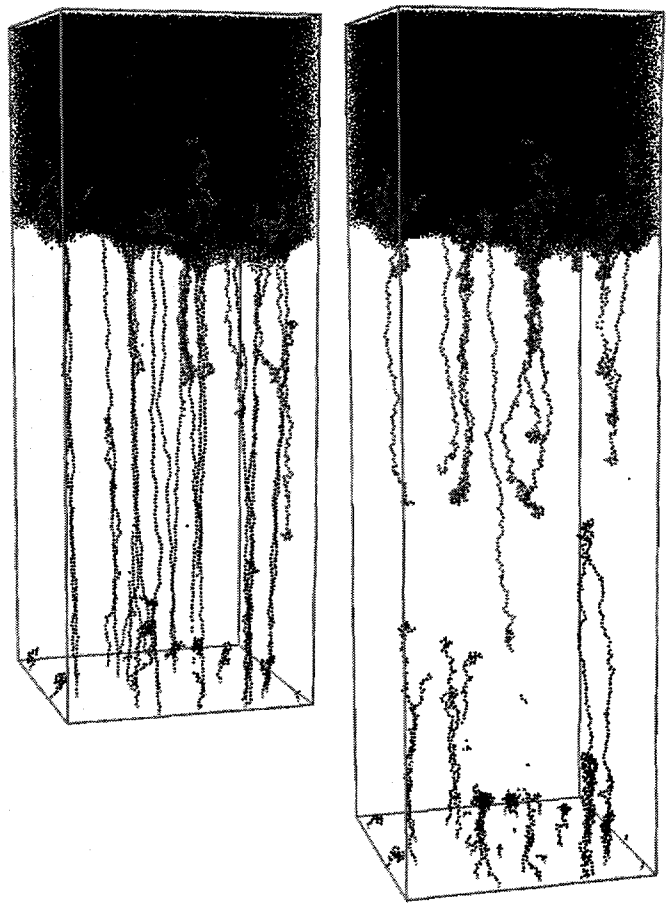

DISCLAIMER